

Quantum Treatment of Continuum Electrons in the Fields of Moving Charges

Teck-Ghee Lee,^{1, 2,*} S. Yu. Ovchinnikov,^{1, 3} J. Sternberg,³ V. Chupryna,³ D. R. Schultz,¹ and J. H. Macek^{1, 3}

¹*Physics Division, Oak Ridge National Laboratory, Oak Ridge, TN 37831*

²*Department of Physics and Astronomy, University of Kentucky, Lexington, KY 40506*

³*Department of Physics and Astronomy, University of Tennessee, Knoxville, TN 37496*

(Dated: February 5, 2008)

An *ab initio*, three-dimensional quantum mechanical calculation has been performed for the time-evolution of continuum electrons in the fields of moving charges. Here the essential singularity associated with the diverging phase factor in the continuum wave function is identified and removed analytically. As a result, the continuum components of the regularized wave function are slowly varying with time. Therefore, one can propagate continuum electrons to asymptotically large times and obtain numerically stable, well-converged ejected electron momentum spectra with very low numerical noise. As a consequence, our approach resolves outstanding controversies concerning structures in electron momentum distributions. The main conclusions are general and are illustrated here for ionization of atomic hydrogen by proton impact. Our results show that in order to obtain correct long-time free-particle propagation, the essential singularity identified here should be removed from the continuum components of solutions to the time-dependent Schrödinger equation.

PACS numbers: 34.70.+e, 34.50.Pi

Tracing the evolution of continuum electrons in the presence of time-dependent external fields as they move from microscopic to macroscopic distances has been of great fundamental interest since the beginning of quantum mechanics [1]. Observations are made at distances where they can be detected by devices such as photon or particle detectors which also have macroscopic dimensions. Substantial progress has been made in the measurements of continuum electrons owing to the development of the cold target recoil ion momentum spectroscopy technique [2, 3, 4, 5], for example. We describe a corresponding theoretical advance in this Letter. This advance is made possible by combining two lines of research, namely, the lattice time-dependent Schrödinger equation (LTDSE) method of Schultz and coworkers [6, 7, 8] and the removal of essential singularities of continuum wave packets described in this Letter but implicit in the dynamical Sturmian theory of Ovchinnikov and coworkers [9].

Although standard numerical techniques successfully apply for time-dependent Schrödinger equation (TDSE) of bound states, they meet with many difficulties for the continuum components due to highly oscillatory phase factors $\exp[i\mathbf{r}^2/2t]$ as is evident from the free-particle propagator (see Eq.(2.5.16) in Ref.[1]). Because these phase factors have essential singularities for large distances, both fundamental and numerical difficulties arise. Even with today's most powerful computers, propagation to large times without accurate treatment of the essential singularity is not possible. Here we present a technique to remove the singularity and apply it to a prototypical system treated in an explicitly time-dependent approach. To the best of our knowledge, no standard numerical methods exist that can rigorously compute the time-evolution of quantum systems from atomic to macroscopic scales.

With removal of the essential singularity, accurate numerical solution of the TDSE to asymptotically large times becomes possible. This is important for physical processes where electron motion at large times, in contrast to just near the parent nuclei, plays a decisive role. For example, in ion-atom collisions, classical trajectory Monte Carlo calculations [10] show that cusps in the ejected electron spectra do not emerge until the target and projectile species are separated by more than 5,000 a.u., many times larger than the initial atomic dimensions. Moreover, cusps are known on fundamental grounds to occur and are prominent features of all ionization processes where nuclear charges are not completely screened in the final state. For ionization by strong laser fields, rescattering of electrons from atomic or molecular species is important for multiple ionization and high harmonic generation [11]. Such rescattering occurs due to oscillations of the laser field so that the electron periodically turns around at large distances and recollides with the core of the species from which it originated.

Thus, the key innovation illustrated in the present work is of far-reaching importance because the motion of continuum electrons in external fields is central to many processes which have only been treated classically until now. Specifically, we show how to treat these processes on an *ab initio*, completely quantum mechanical basis. To begin with, the electronic wave function is written in the form (atomic units are used throughout the paper unless otherwise indicated)

$$\Psi(\mathbf{r}, t) = \chi(\mathbf{q}, \theta)\Phi(\mathbf{q}, \theta), \quad (1)$$

where $\mathbf{q}=(\mathbf{r}v \sin \theta)/\Omega$ and $t=-(\Omega \cot \theta)/v^2$, θ varies from 0 to π , and v and Ω are arbitrary parameters in general

but later v will represent a physical velocity. The factor

$$\chi(\mathbf{q}, \theta) = \left(\frac{i \sin \theta}{\Omega} \right)^{3/2} \exp[-i(\Omega q^2 \cot \theta)/2] \quad (2)$$

is highly oscillatory and has an essential singularity at $1/q=0$ (*i.e.* $q \rightarrow \infty$).

The *regularized* wave function $\Phi(\mathbf{q}, \theta)$ however, has slow-varying continuum components and satisfies a regularized time-dependent Schrödinger equation (RTDSE)

$$\left[-\frac{1}{2} \nabla_{\mathbf{q}}^2 + \frac{1}{2} \Omega^2 q^2 + V(\mathbf{q}, \theta) \right] \Phi(\mathbf{q}, \theta) = i\Omega \frac{\partial \Phi(\mathbf{q}, \theta)}{\partial \theta}, \quad (3)$$

where $V(\mathbf{q}, \theta)$ is an external, possibly time-dependent, potential. Time-dependent scale-transformations have been used to solve a model problem exactly [12] and a one dimension problem numerically [13], but the method introduced here enables efficient and full numerical calculations.

In the present application where the bare projectile of charge Z_P collides with a one-electron target of nuclear charge Z_T , the interaction is given by

$$V(\mathbf{q}, \theta) = \frac{\Omega}{v \sin \theta} \left(-\frac{Z_P}{|\mathbf{q} + \mathbf{Q}(\theta)/2|} - \frac{Z_T}{|\mathbf{q} - \mathbf{Q}(\theta)/2|} \right) \quad (4)$$

where $\mathbf{Q}(\theta)$ can represent any trajectory. Here we use a straight-line trajectory to describe the nuclear motion, *i.e.* $\mathbf{Q}(\theta) = \cos \theta \hat{\mathbf{v}} + v b \sin \theta \hat{\mathbf{b}}/\Omega$, where v is now the relative velocity and b is the impact parameter.

The initial regularized wave function is given by

$$\Phi_0(\mathbf{q}, \theta_0) = \frac{\Psi_0(v^{-1} \mathbf{q}, \Omega \csc \theta_0, -v^{-2} \Omega \cot \theta_0)}{\chi(\mathbf{q}, \theta_0)}, \quad (5)$$

where $\Psi_0(\mathbf{r}, t_0)$ is the full wave function at the initial time $t_0 = -(\Omega \cot \theta_0)/v^2$. At asymptotically large times as $\theta \rightarrow \pi$, the continuum components of $\Phi(\mathbf{q}, \theta)$ are independent of Ω and directly give the ejected electron momentum distributions [9]

$$A(\mathbf{k}) = \lim_{\theta \rightarrow \pi} \Phi(\mathbf{q}, \theta), \quad (6)$$

where $\mathbf{q} \rightarrow \mathbf{k}/v$ in the limit and \mathbf{k} is the electron wave vector. Note that the present formulation does not require projection onto dynamic two-center continuum states at large times since the bound states shrink to vanishingly small regions in \mathbf{q} -space. Eq. (3) can be then solved using a number of different numerical methods.

We compute the ejected electron spectra for proton impact ionization of hydrogen atoms in the impact energy

range of 5–25 keV where there are long standing controversies regarding the momentum distribution of ejected electrons [5, 8, 14]. Owing to its numerical accuracy and efficiency we adopt here the LTDSE technique [6, 7, 8]. As the two moving charges become separated by a very large distance, the electronic probability density in the continuum becomes infinitesimally small, spread over an enormous spatial volume. As a result, previous calculations have always terminated at relatively small distances on the order of 30 to 100 a.u. [7, 8, 14] before the continuum electron density becomes so small that it poses intractable numerical difficulties.

Because of the present singularity-free, scaled representation, the RTDSE does not suffer from this impediment. Furthermore, due to the steep walls of the harmonic oscillator potential in Eq. (3), reflections at the lattice boundaries are inherently insignificant. Finally, removing the essential singularity also allows us to integrate along a path in the complex θ –plane where the interaction potential never vanishes for real \mathbf{q} , allowing us to avoid conventional, *ad hoc* softcore modifications of the potentials near the Coulomb singularities.

Regarding specific parameters of the present calculations, we choose $\Omega \approx 1$ and the scaled box size $|q_i| \leq 7$, $i = x, y, z$ with 256^3 points in order to minimize the level of numerical noise in the resulting electron momentum distributions. This is judged by performing a test calculation with projectile charge set to zero. Using the quantity $1 - |\langle \Phi(\theta) | \Phi_0(\theta) \rangle|^2$ as measure of the noise, we find it to be less than 3×10^{-7} . This error is small enough so that all of the momentum distribution within a box $|k/v| < 2.5$ (*e.g.*, see Fig.1) is numerically significant. Such small and controllable errors set a standard for accuracy of full 3-dimensional numerical solutions of the TDSE and allow us to see features of electron distributions that are beyond the previous state-of-the-art.

We begin by noting that in this energy range considered here, ionization occurs via transfer of energy from nuclear to electronic motion in regions where there are periodic, unstable classical trajectories. There are two types of these trajectories, namely, the superpromotion (S) trajectories along the internuclear axis (*e.g.*, as in the Fermi Shuttle mechanism [15]), and the top-of-barrier (T) trajectories where the electron moves perpendicular to the axis joining the nuclei near the region where the net force on the electron vanishes. The S-type motion is effective as the nuclei approach while the T-type is effective as they recede. Both types of trajectories are related to quantal transitions between H_2^+ –like adiabatic molecular energy curves [16].

Figure 1 shows 2-dimensional slices of the ejected electron

momentum (or wave vector \mathbf{k}) distributions taken with

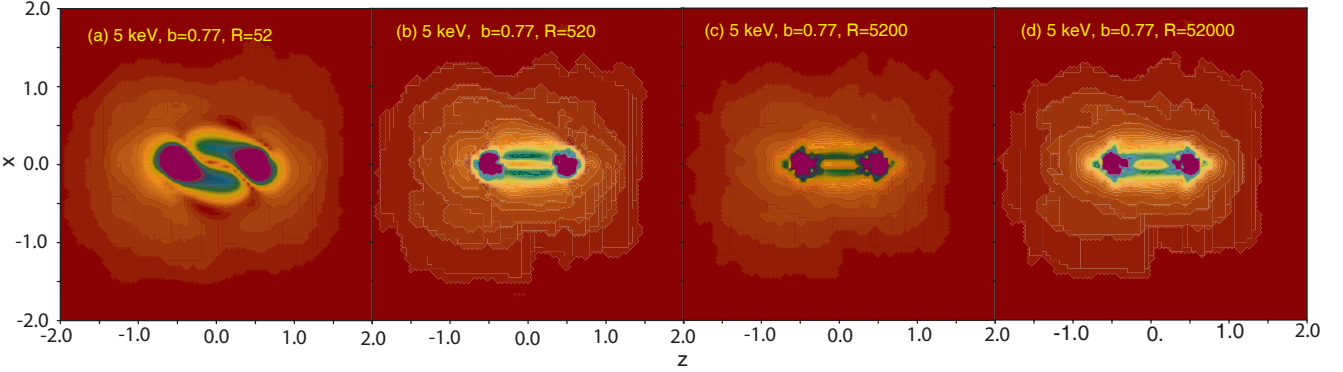


FIG. 1: The time-evolution of the spectrum of ejected electrons at a collision energy of 5 keV and an impact parameter of $b=0.77$ a.u. for proton impact ionization of hydrogen. The time integration is terminated at 4 internuclear separations: (a) $R=52$ a.u., (b) $R=520$ a.u., (c) $R=5,200$ a.u. and (d) $R=52,000$ a.u. The electronic amplitude (Eq. (6)) has values of ~ 0.02 near the edges of the distribution and ~ 0.64 a.u. at $q_x=0$ and $q_z=\pm 0.5$. Note that the electron wave vector \mathbf{k} is measured in units of the relative ion velocity v .

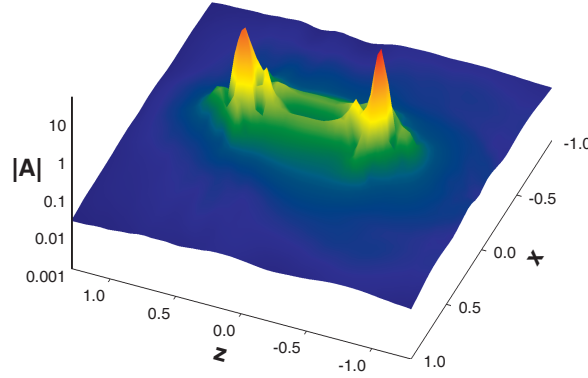


FIG. 2: Plot of the ionization amplitude $|A|$ of Eq. (6) showing target and projectile cusps with the bound states removed.

the q_z -axis parallel to the projectile velocity \mathbf{v} , the q_x -axis parallel to the impact parameter \mathbf{b} and y equal to zero, computed for collision energy 5 keV with $b=0.77$ a.u., and with the time integration terminated at four internuclear separations: $R = 52, 520, 5,200$ and $52,000$ a.u. One can see that the distribution changes significantly between 52 and 5,200 a.u., predicted in a special limiting case [17], with a small, but noticeable, change between 5,200 and 52,000 a.u.

At all post-collisional internuclear distances there are fast electrons, *i.e.* electrons with velocities greater than the projectile velocity v , distributed approximately isotropically about the center of mass. These electrons originate from two S-type transitions near $R=0.4$ a.u. and $R=1$ a.u. The electrons are distributed in angle according to the angular part of the adiabatic H_2^+ wave function at complex values of the internuclear distance R [17]. The relevant angular parts have not been reported in the literature, but they are assumed to be given

in terms of spherical harmonics with relatively low values of angular momentum ℓ . This agrees qualitatively with the *ab initio* distributions reported here.

The ‘elliptical’ ring of electrons between the target and projectile is another remarkable feature which becomes narrower as R increases, and can be interpreted in terms of T-type transitions, *i.e.* electrons are ejected by a process that involves a united-atom rotational coupling transition followed by T-promotion to the continuum. It is known that united-atom rotational coupling produces a state of π symmetry with a node along the internuclear axis. The shape of this feature at $R=52$ a.u. and its narrowing for increasing R support this interpretation.

Electron cusps at $\mathbf{k}=\pm\hat{\mathbf{v}}/2$ are also seen in Fig. 1, although one must remember that the bound state electrons are not separated from the cusps in this figure. It is necessary to extrapolate the distribution to small \mathbf{k} when R is asymptotically large in order to identify these features correctly. Figure 2 shows the ionization amplitude $|A|$ at $R=52,000$ a.u. The electrons in the cusps are a small fraction of the total that are ejected, however, even this small component can be identified with the theoretical approach that we report here for the first time with such a time-dependent grid approach.

The identification of these features is supported by the distributions shown in Fig. 3 for increasing projectile velocity. Note that the superpromotion features shrink in extent but do not change shape. This is in accord with predictions of an exponential $\exp[-0.4(k/v)^2 v]$ distribution [9]. Alternatively, the T-electron distribution retains the same spatial extent but oscillates as identified in Ref. [9]. In contrast with that earlier approximate theory, it can be seen that some of the electrons actually move from the center to the target and projectile nuclei. Note that all of the features identified here are superimposed co-

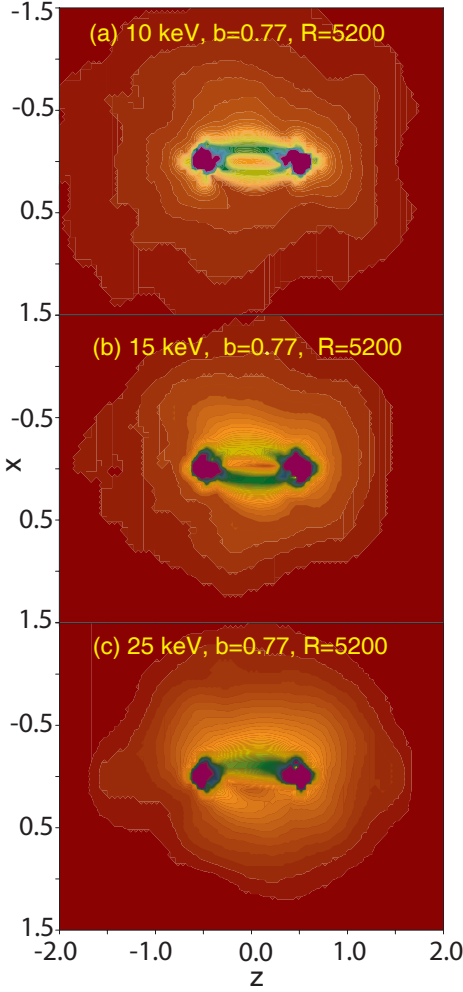


FIG. 3: Same as in Fig. 1 but for higher collision energies with $R=5,200$ a.u . The amplitude ranges from ~ 0.04 near the edges of the distributions to ~ 1.36 a.u. at $q_x=0$ and $q_z=\pm 0.5$.

herently so that interference effects may emerge. Indeed, interference structure near the cusps in Fig. 2 is apparent. A more detailed analysis of the time-dependent wave functions shows that the S-type electrons interfere with the T-type electrons that have moved from the midpoint of the internuclear axis. Such interference has not been noted previously since a coherent treatment of S- and T-type processes has been beyond the reach of theory.

The most important conclusion from the present calculations is that, even for the many-faceted electron distributions seen in Figs. 1-3, in experiment, and in earlier calculations [9], the overall phase factor of the electronic wave function in continuum is given by Eq. (2). In $\{\mathbf{r}, t\}$ -space this factor for $R \gg 1$ is just $\exp[i\mathbf{r}^2/2t]$ as derived from the free electron propagator. With this phase factor removed, a regularized Schrödinger equation is obtained

that is solved efficiently using the LTDSE method. This has allowed us to develop a general theoretical approach that allows one to solve the time-dependent Schrödinger equation from microscopic to macroscopic distances accurately. The method is well-suited for treating continuum electrons in time-dependent fields. Computations of ejected electron distributions produced by proton impact on atomic hydrogen have been used here to illustrate the method. The results show measurable features not amenable to previous theoretical approaches. The features are in qualitative accord with electron distributions measured for proton impact on helium [2].

This research is sponsored by the Office of Basic Energy Sciences, U.S. Department of Energy, under Contract No. DE-AC05- 96OR22464 through a grant to Oak Ridge National Laboratory, which is managed by UT-Battelle, LLC under Contract No. DE-AC05-00OR22725. JHM, SYO and JS, acknowledge support by DOE grant DE-FG02-02ER15283 to the University of Tennessee. TGL acknowledges support by NASA grant NNG05GD81G to the University of Kentucky.

* Corresponding author email: leetg@ornl.gov

- [1] J. J. Sakurai, *Modern Quantum Mechanics* (Addison-Wesley, 1994) p112.
- [2] R. Dörner, *et al.*, Phys. Rev. Lett. **77**, 4520 (1996).
- [3] R. Moshammer *et al.*, Phys. Rev. Lett. **87**, 223201-1 (2001).
- [4] M. Schulz *et al.*, Nature, **422**, 48 (2003).
- [5] J. Ullrich, *et al.*, Rep. Prog. Phys. **66**, 1463 (2003).
- [6] J.C. Wells, D.R. Schultz, P. Gavras, and M.S. Pindzola, Phys. Rev. A **54**, 593 (1996).
- [7] D.R. Schultz, M.R. Strayer, and J.C. Wells, Phys. Rev. Lett. **82**, 3976 (1999).
- [8] D. R. Schultz, C. O. Reinholt, P. S. Krstic, and M. R. Strayer, Phys. Rev. A **65**, 052722 (2002).
- [9] J. H. Macek and S. Yu. Ovchinnikov, Phys. Rev. Lett. **80**, 2298 (1998); S. Yu. Ovchinnikov, *et. al.*, Phys. Repts. **389**, 119 (2004).
- [10] C. O. Reinholt and R. E. Olson, Phys. Rev. A **39**, 3861 (1989).
- [11] V. S. Yakovlev and A. Scrinzi, Phys. Rev. Lett **91**, 153901 (2003).
- [12] M. J. Rakovic and E. A. Solov'ev, Phys. Rev. A **41**, 3635 (1990).
- [13] E. Y. Sidky and B. D. Esry, Phys. Rev. Lett. **85**, 5086 (2000).
- [14] E. Y. Sidky and C. D. Lin, Phys. Rev. A **60**, 377 (1999).
- [15] B. Sulik, Cs. Koncz, K. Toksi, A. Orbn, and D. Bernyi , Phys. Rev. Lett. **88**, 073201 (2002).
- [16] M. Pieksma and S. Yu. Ovchinnikov, J. Phys. B **27**, 4573 (1994).
- [17] S. Yu. Ovchinnikov and J. H. Macek, Phys. Rev. Lett. **75**, 2474 (1995).